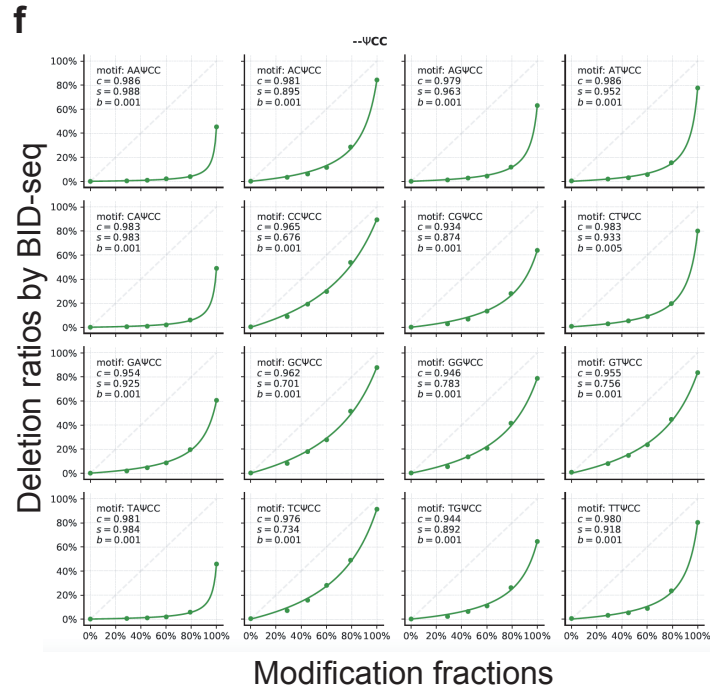
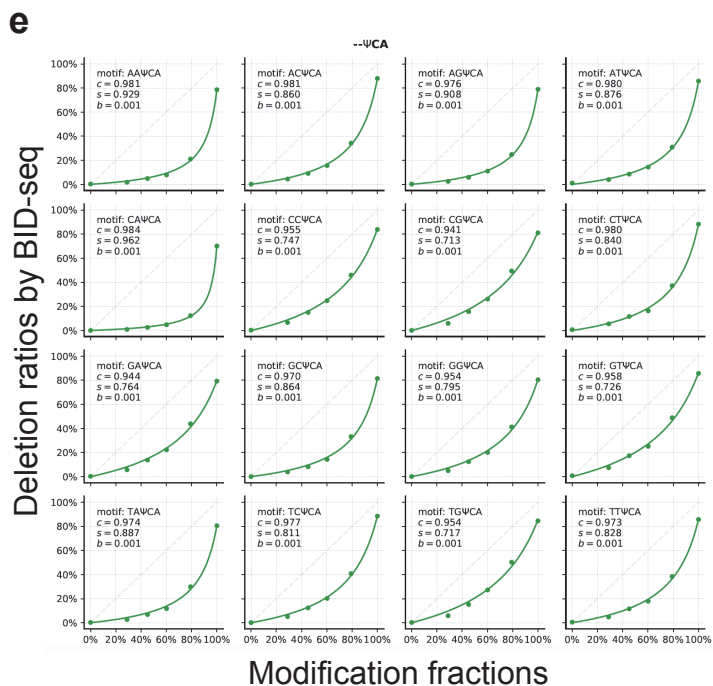
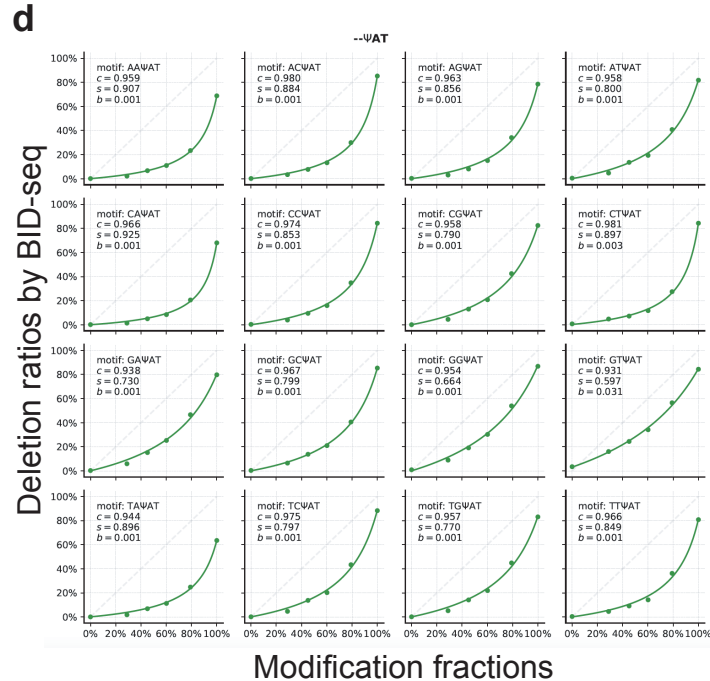
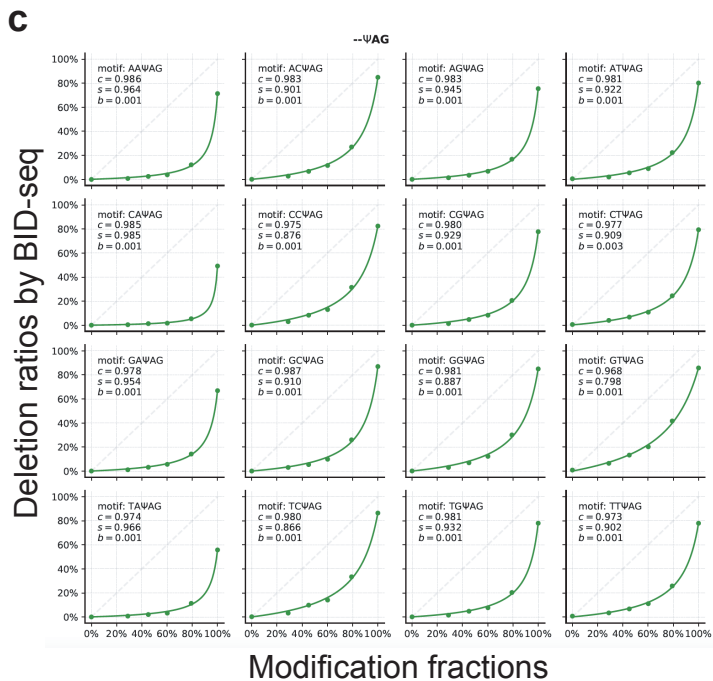
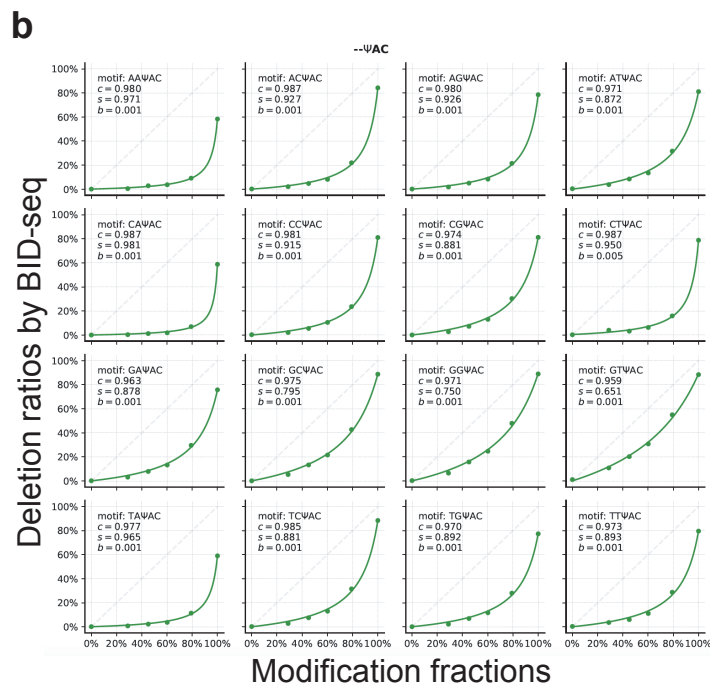
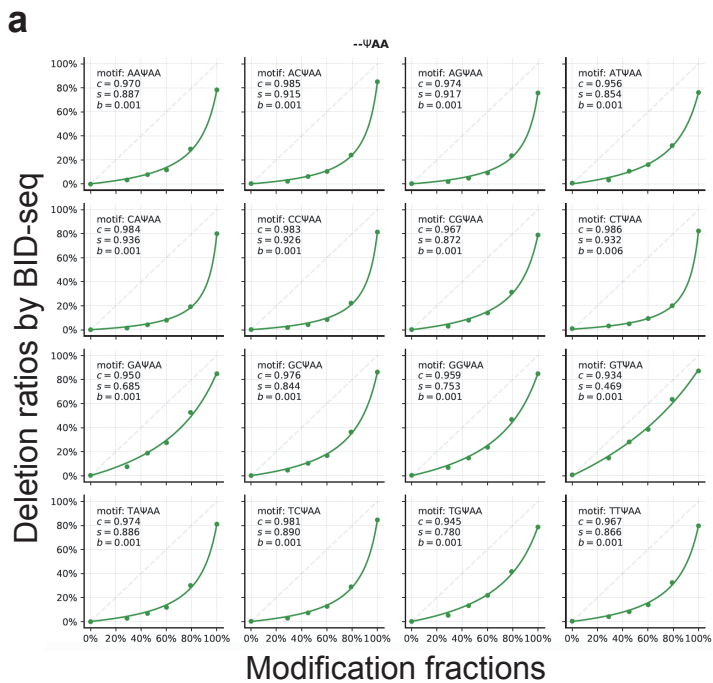
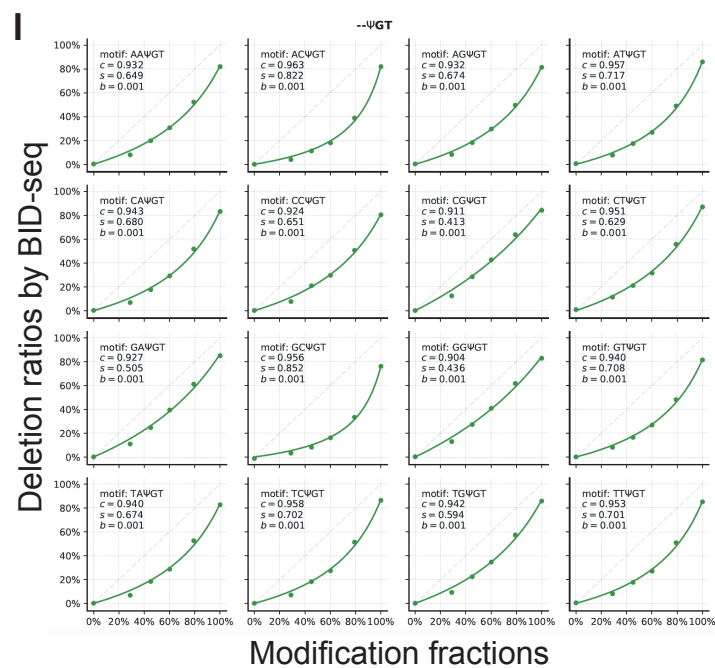
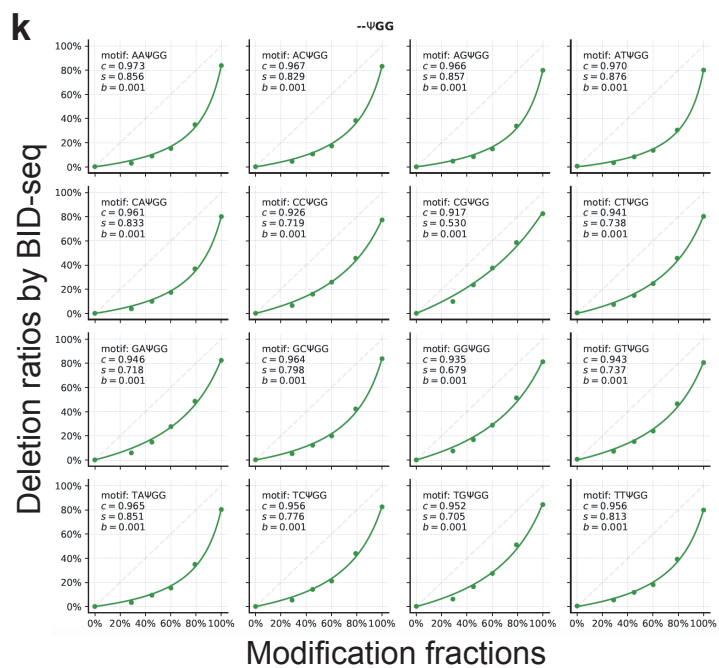
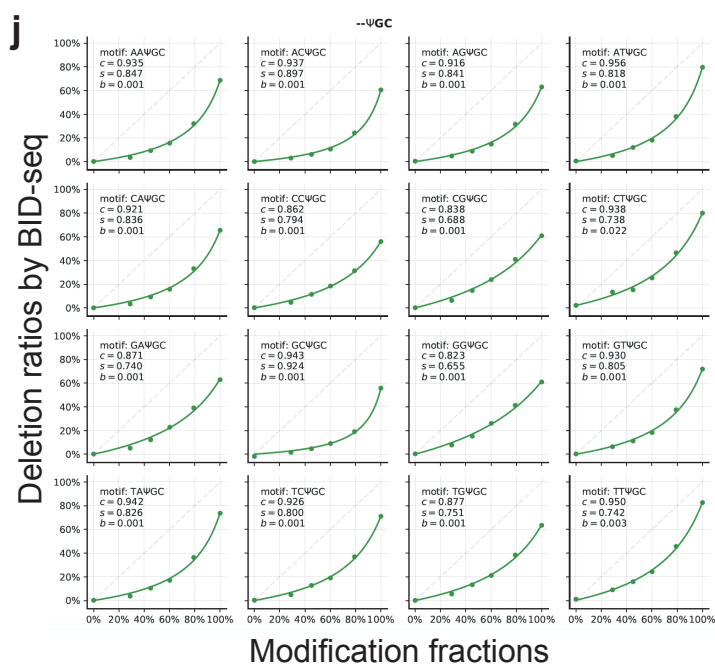
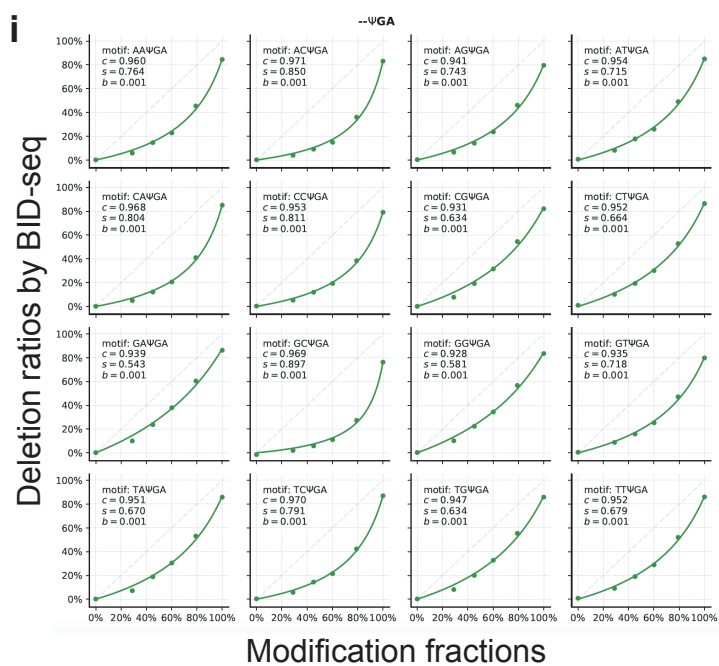
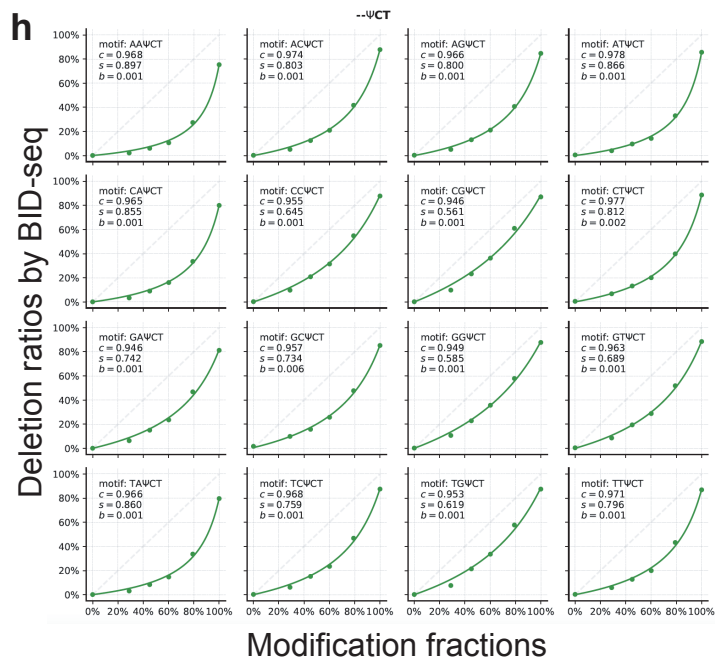
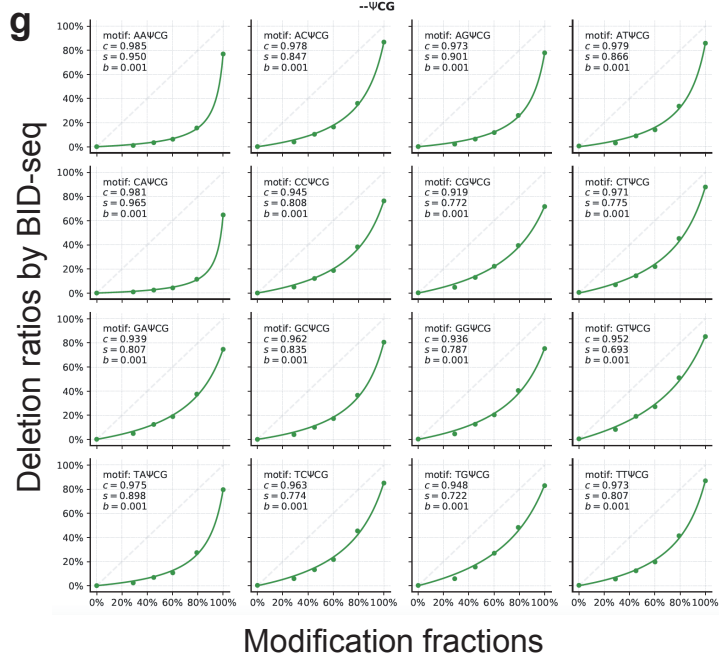
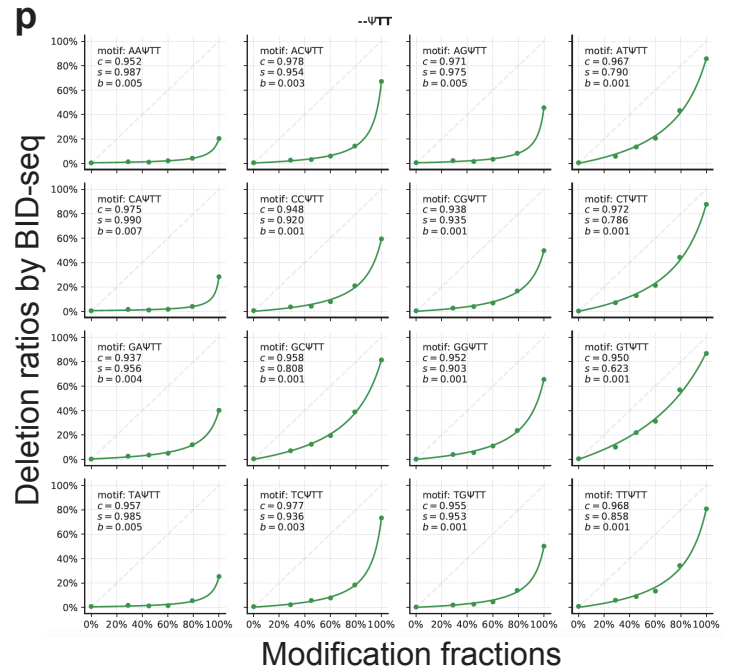
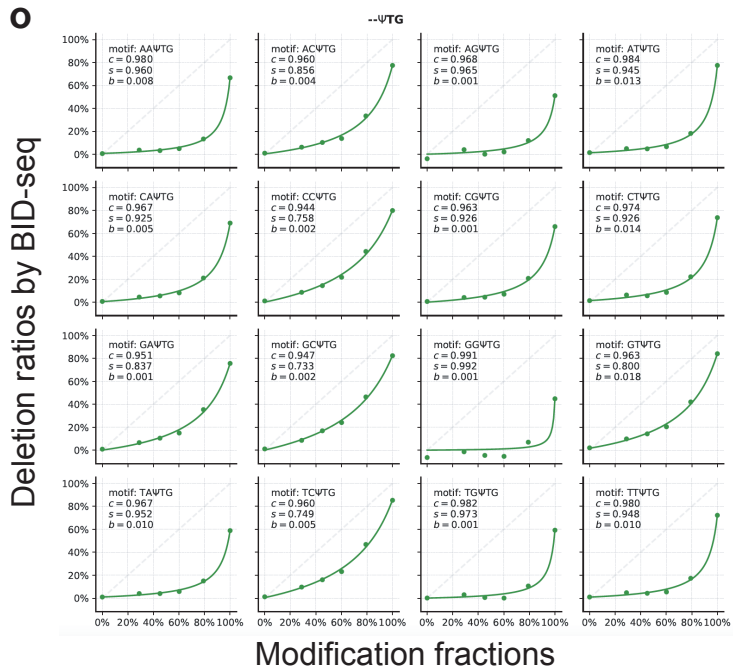
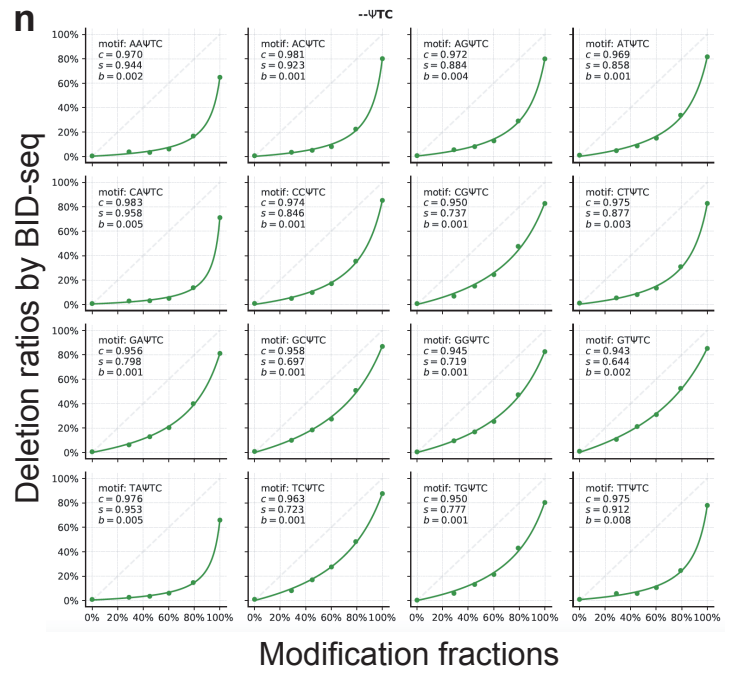
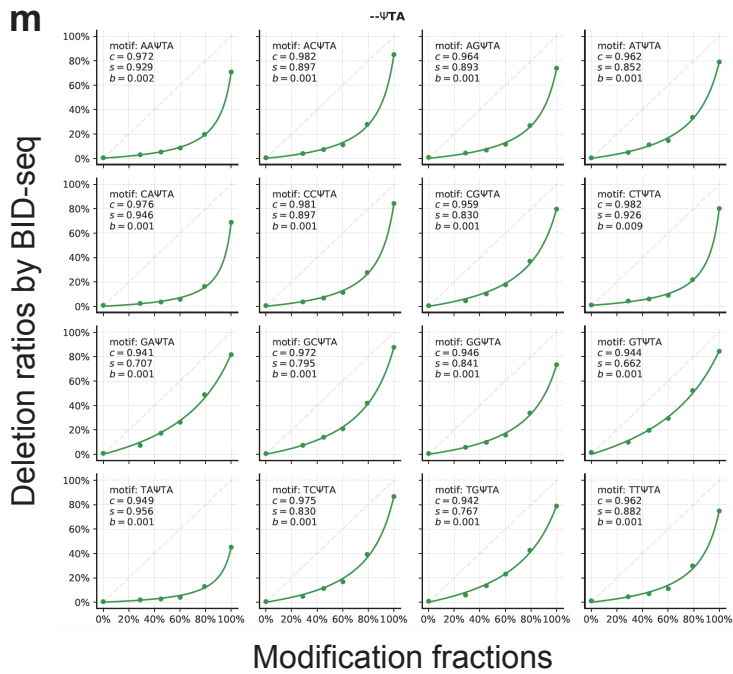


BID-seq for transcriptome-wide quantitative sequencing of mRNA pseudouridine at base resolution

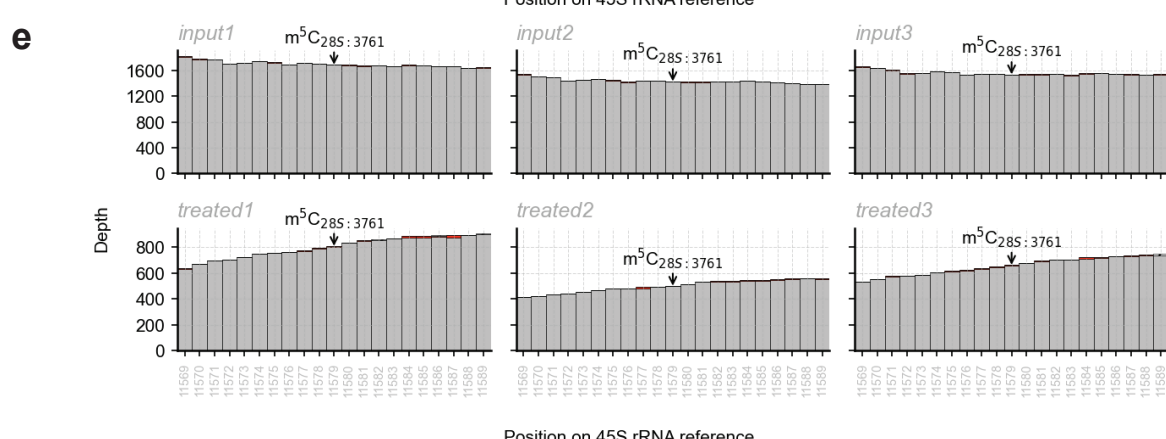
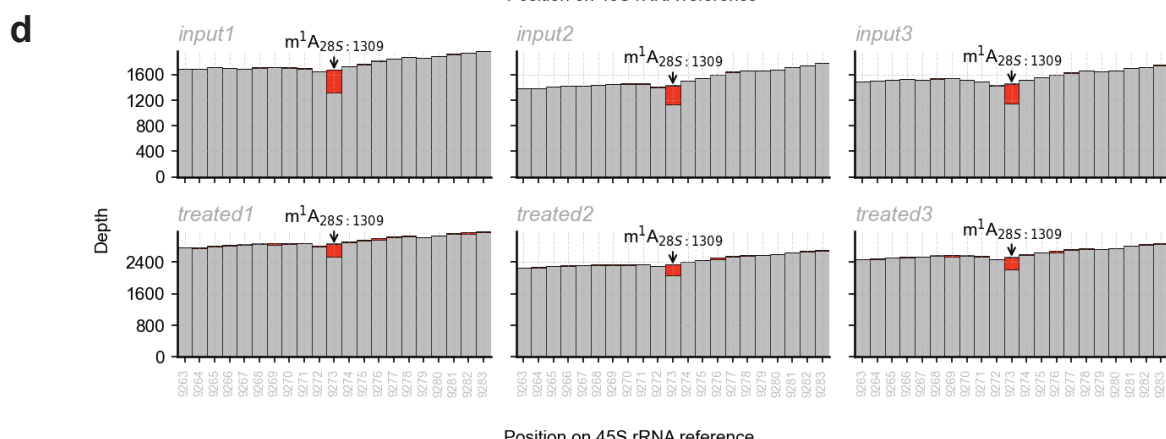
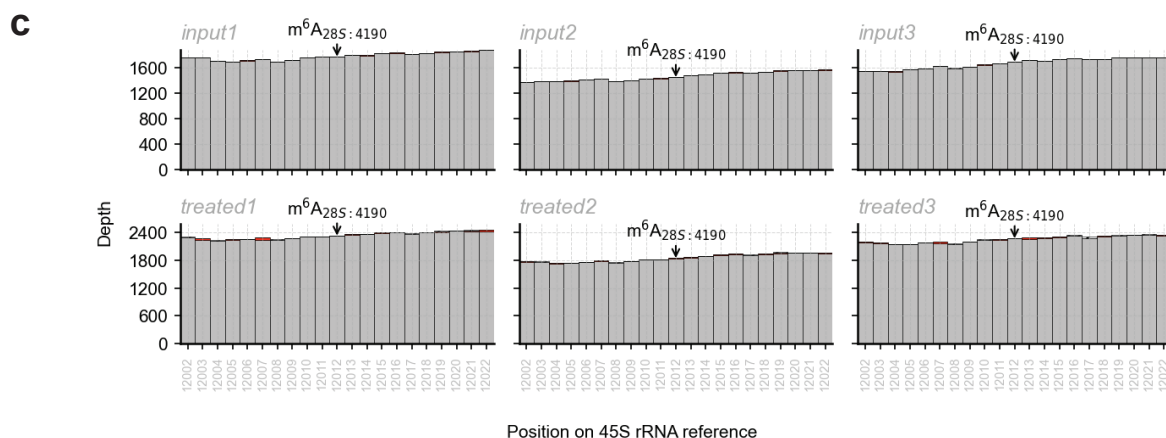
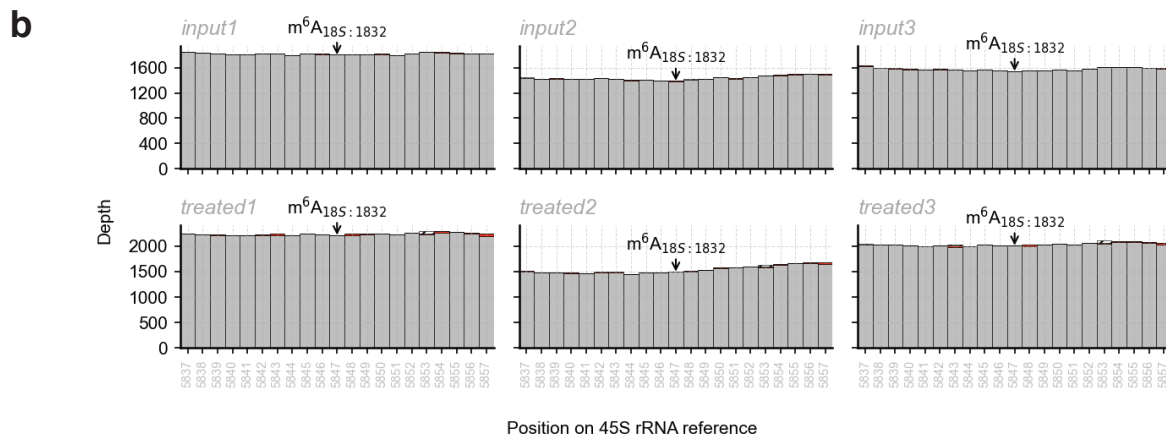
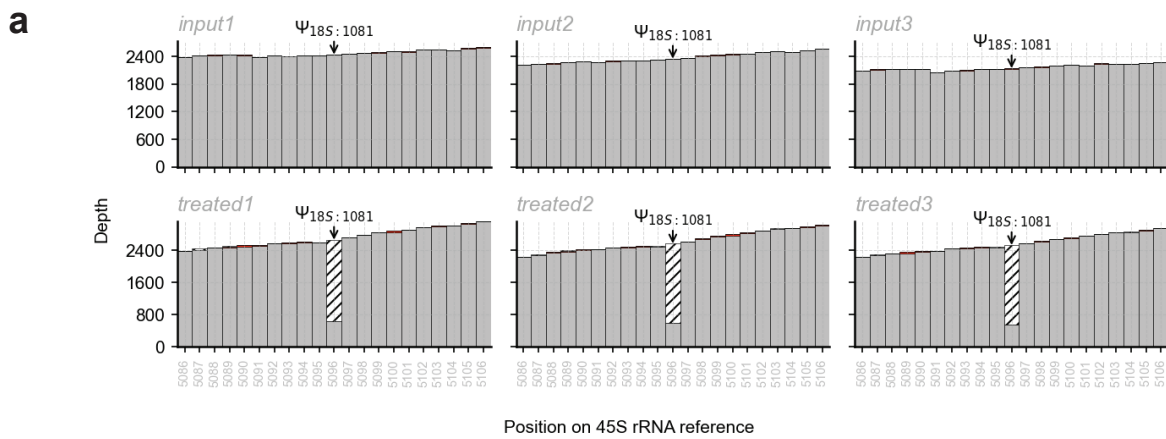
In the format provided by the authors and unedited

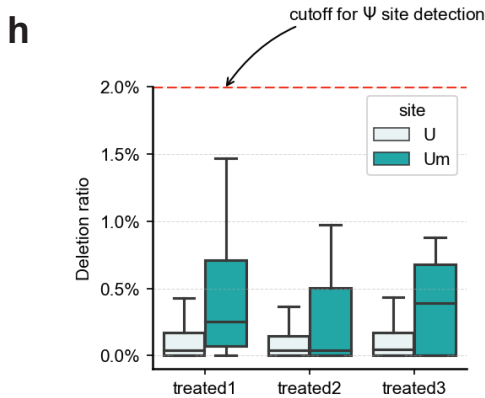
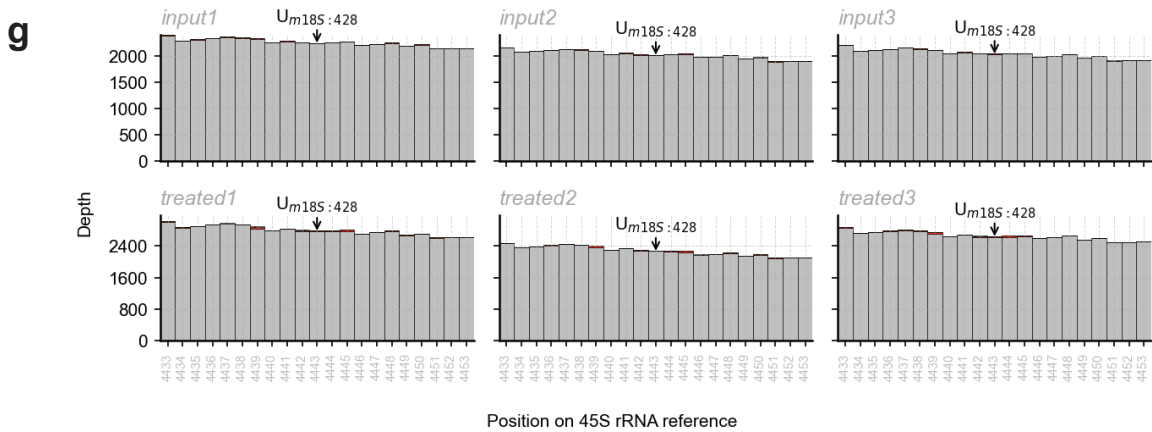
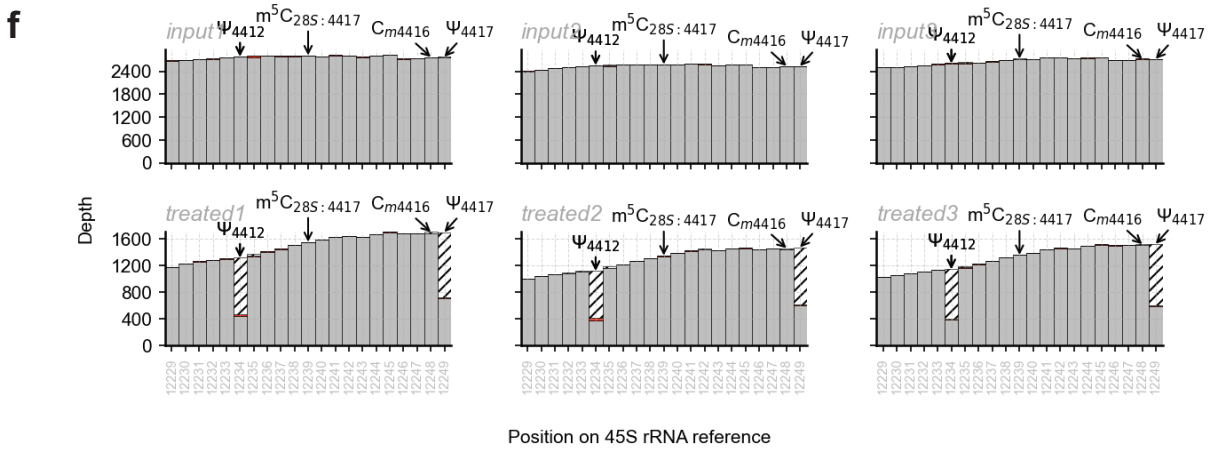




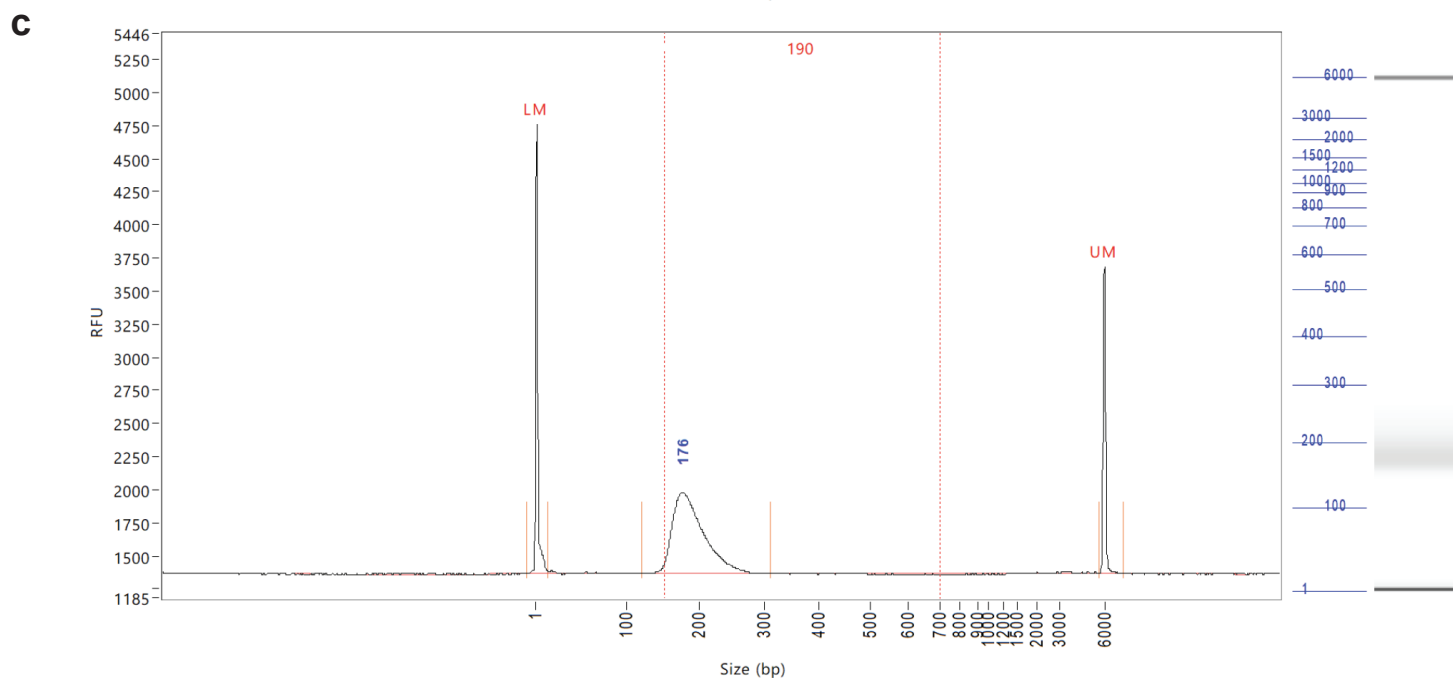
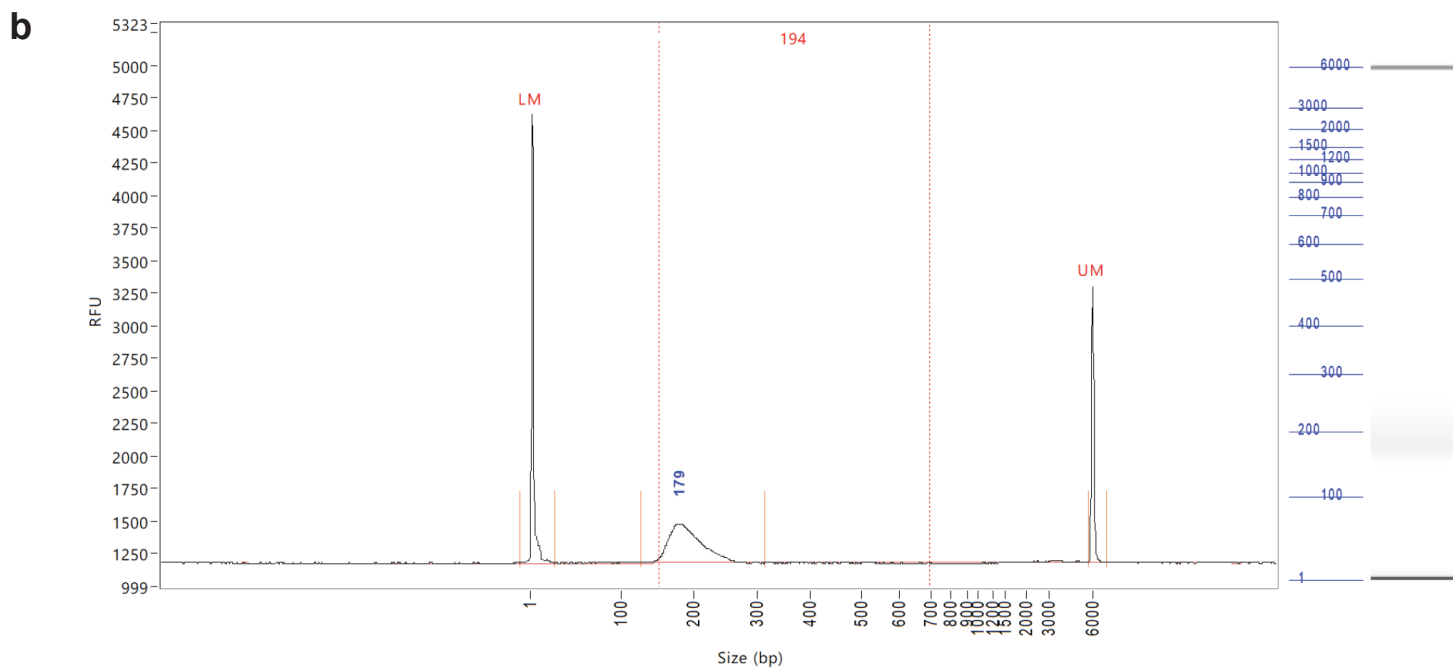
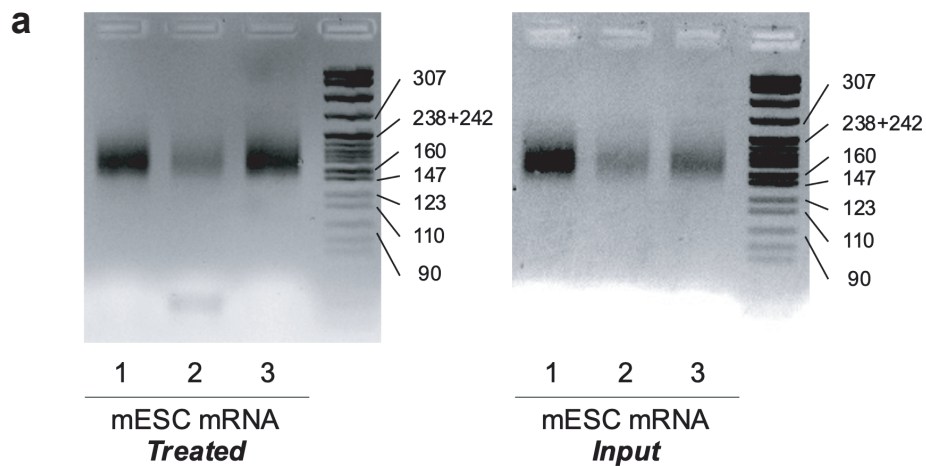


Supplementary Fig. 1 | The calibration curves for BID-seq, based on BID-pipe analysis. a, The BID-seq calibration curves for motif contexts containing NN- Ψ AA. b, The BID-seq calibration curves for motif contexts containing NN- Ψ AC. c, The BID-seq calibration curves for motif contexts containing NN- Ψ AG. d, The BID-seq calibration curves for motif contexts containing NN- Ψ AU. e, The BID-seq calibration curves for motif contexts containing NN- Ψ CA. f, The BID-seq calibration curves for motif contexts containing NN- Ψ CC. g, The BID-seq calibration curves for motif contexts containing NN- Ψ CG. h, The BID-seq calibration curves for motif contexts containing NN- Ψ CU. i, The BID-seq calibration curves for motif contexts containing NN- Ψ GA. j, The BID-seq calibration curves for motif contexts containing NN- Ψ GC. k, The BID-seq calibration curves for motif contexts containing NN- Ψ GG. l, The BID-seq calibration curves for motif contexts containing NN- Ψ GU. m, The BID-seq calibration curves for motif contexts containing NN- Ψ UA. n, The BID-seq calibration curves for motif contexts containing NN- Ψ UC. o, The BID-seq calibration curves for motif contexts containing NN- Ψ UG. p, The BID-seq calibration curves for motif contexts containing NN- Ψ UU.





Supplementary Fig. 2 | The deletion profiles of SuperScript IV RT at different RNA modifications on mESC rRNA. a, BID-seq reveals dramatic deletion signatures at Ψ_{1081} of mESC 18S rRNA. **b**, BID-seq does not reveal any deletion signatures at m^6A_{1832} of mESC 18S rRNA. **c**, BID-seq does not reveal any deletion signatures at m^6A_{4190} of mESC 28S rRNA. **d**, BID-seq does not reveal any deletion signatures at m^1A_{1309} of mESC 28S rRNA. **e**, BID-seq does not reveal any deletion signatures at m^5C_{3761} of mESC 28S rRNA. **f**, BID-seq does not reveal any deletion signatures at m^5C_{4417} of mESC 28S rRNA. **g**, BID-seq does not reveal any deletion signatures at U_{m428} of mESC 18S rRNA. **h**, For all Um sites on mESC rRNA, the deletion ratios at Um sites are much lower than Ψ detection cutoff in BID-pipe.



Supplementary Fig. 3 | The Agarose gel and Bioanalyzer plot to show the size of BID-seq libraries. a, The agarose gel image to show the sizes of 'Input' and 'Treated' libraries built with mESC polyA⁺ RNA, in BID-seq. **b,** The Bioanalyzer measurement to show the size of 'Input' library built with mESC polyA⁺ RNA, in BID-seq. **c,** The Bioanalyzer measurement to show the size of 'Treated' library built with mESC polyA⁺ RNA, in BID-seq.